AGU PUBLICATIONS

JGR

Journal of Geophysical Research: Solid Earth

RESEARCH ARTICLE
10.1002/2015JB011881

Key Points:
- Wet smectite-quartz mixed gouges show intermediate velocity weakening
- The weakening results from fluid pressurization and impermeable gouge
- Low- to high-velocity slip behavior of gouges depends on smectite content

Correspondence to:
K. Oohashi,
oohashik@yamaguchi-u.ac.jp

Citation:
Oohashi, K., T. Hirose, M. Takahashi, and W. Tanikawa (2015), Dynamic weakening of smectite-bearing faults at intermediate velocities: Implications for subduction zone earthquakes, *J. Geophys. Res. Solid Earth*, *120*, doi:10.1002/2015JB011881.

Received 8 JAN 2015
Accepted 18 FEB 2015
Accepted article online 24 FEB 2015

Dynamic weakening of smectite-bearing faults at intermediate velocities: Implications for subduction zone earthquakes

Kiyokazu Oohashi[1], Takehiro Hirose[2], Miki Takahashi[3], and Wataru Tanikawa[2]

[1]Department of Earth Science, Graduate School of Science and Engineering, Yamaguchi University, Yamaguchi, Japan, [2]Kochi Institute for Core Sample Research, Japan Agency for Marine–Earth Science and Technology, Kochi, Japan, [3]Active Fault and Earthquake Research Center, National Institute of Advanced Industrial Science and Technology, Tsukuba, Japan

Abstract The hydrous clay mineral smectite, which is pervasive in sediments on subducting oceanic plates, is thought to weaken and stabilize subduction thrust faults. However, these frictional properties of smectite alone cannot explain the large coseismic slip in the vicinity of a trench. Here we performed friction experiments to demonstrate the rate dependence of friction at slip rates from 30 μm/s to 1.3 m/s for water-saturated smectite-quartz mixtures with various smectite contents, so as to shed light on the frictional response of smectite-bearing faults at intermediate to high slip rates. At slip rates of 30 to 150 μm/s, the friction coefficients decreased gradually from 0.5–0.6 to 0.1 with an increase in smectite content from 20 to 50 wt %. In contrast, at slip rates higher than 1.3 mm/s, friction exhibited marked slip weakening, resulting in low friction coefficients of 0.1–0.05, even for low smectite contents (roughly $<$30 wt %). Drastic slip weakening occurred at smectite contents of 10–30 wt % at slip rates of ~10 mm/s, which is 1 to 2 orders of magnitude lower than the slip rate at which slip weakening was observed in previous experiments on various rock types. The intermediate velocity weakening could be attributed to a rise in pore pressure caused by both shear-enhanced compaction and microscopic thermal pressurization of pore fluids. This process could weaken the fault even below seismic slip rates, leading to an acceleration of fault motion and potentially facilitating large coseismic slip and a stress drop in the vicinity of a trench.

1. Introduction

Shallow portions of subduction zone thrust faults have been considered to be aseismic given the observed absence of seismicity in such regions [e.g., *Hyndman et al*., 1997]. The velocity-strengthening property of friction for clay-rich sediments is thought to explain aseismic creep behavior at the shallow plate boundaries of subduction zones [*Saffer and Marone*, 2003]. However, unexpectedly large coseismic slip occurred at the shallow plate interface during the 2011 Tohoku Earthquake [e.g., *Fujiwara et al*., 2011]. Tsunami inversions [*Cummins and Kaneda*, 2000] and the signals of frictional heat, possibly due to coseismic sliding detected from the shallow portions of subduction thrusts [*Sakaguchi et al*., 2011; *Yamaguchi et al*., 2011], also suggest that earthquake ruptures could have propagated updip from deep seismogenic zones to near the seafloor in the Nankai subduction zone. Although several processes (such as the state of stress [e.g., *Kozdon and Dunham*, 2013] and the presence of a fluid overpressure zone [e.g., *Park et al*., 2014]) have been proposed to explain coseismic slip along shallow portions of subduction thrusts, here we focus on the frictional and hydrological properties of subduction zone materials that potentially govern fault behavior in the shallow portions of subduction zones.

Smectite, a hydrous clay mineral, is widely distributed in fore-arc basins and in incoming sediments on subducting oceanic plates in varying amounts, depending on the lithology, depositional age, and the geothermal regime [e.g., *Oinuma and Kobayashi*, 1966; *Cole and Shaw*, 1983]. Smectite contents ranging from 10 to $>$50 wt % have been recorded in the bulk fractions of sediments in the vicinity of the Nankai Trough [e.g., *Guo and Underwood*, 2012]. With respect to frictional properties, smectite is peculiar in its combined weakness and stability [e.g., *Kenney*, 1967; *Summers and Byerlee*, 1977]. Friction experiments on smectite and on smectite-quartz mixtures have previously been conducted using a biaxial or triaxial deformation apparatus under low slip rates (mainly 0.1–100 μm/s) to demonstrate how frictional strength decreases with increasing smectite content [*Logan and Rauenzahn*, 1987; *Brown et al*., 2003; *Takahashi et al*., 2007; *Tembe et al*., 2010]. Recent high-velocity friction experiments and theoretical modeling studies have proposed

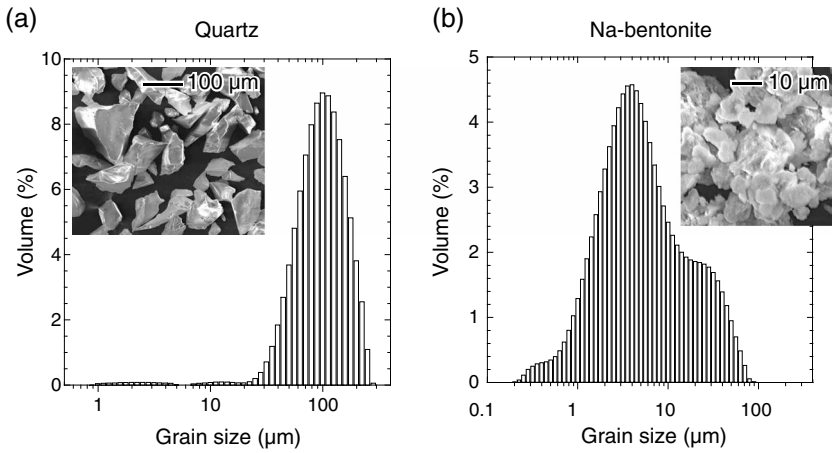

Figure 1. Grain size distributions and scanning electron microscope (SEM) secondary electron images of (a) quartz and (b) Na-bentonite powder. The grain size of the powder was measured by the laser diffraction and scattering method using a commercial particle-size analyzer (Mastersizer2000, Malvern Instruments Ltd.).

dynamic weakening (such as by flash heating, thermal pressurization, frictional melting, and thermal decomposition) to explain large coseismic stress drops [e.g., *Andrews*, 2002; *Hirose and Shimamoto*, 2005; *Rice*, 2006; *Han et al*., 2007]. *Faulkner et al*. [2011] reported dynamic weakening of clay-rich materials, including smectite, based on high-velocity friction experiments (slip rate of about 1.3 m/s), and proposed that rapid thermal pressurization of pore fluid was responsible for the weakening. *Ujiie et al*. [2011] and *French et al*. [2014] also conducted high-velocity friction experiments on smectite-rich, natural fault gouges from the megasplay fault zone in the Nankai subduction zone and the San Andreas Fault, respectively and concluded that pore fluid pressurization to be a weakening mechanism under wet condition. However, the effects of smectite content on the frictional behavior of smectite-quartz mixtures at a wide range of slip rates have still not been quantified in the laboratory.

In this study, we conducted friction experiments for various mixtures of smectite and quartz at low to high slip rates (30 μm/s to 1.3 m/s) under water-saturated conditions, with the aim of understanding the mineralogical dependence of friction over the range of interseismic to coseismic slip rates. We discuss mechanisms for dynamic weakening found under the conditions of relatively slow slip rates and low smectite contents. Our experiments may provide clues regarding the processes of rupture propagation from seismogenic depths to the trench and regarding the generation of tsunamigenic earthquakes in subduction zones.

2. Materials and Methods

2.1. Starting Materials

We used various mixtures of commercially available Na-bentonite powder and quartz (crystalline silica) powder to simulate smectite-bearing fault gouge, without crushing or sieving. The quartz powder was obtained from Wako Pure Chemical Industries Ltd (product number: 199–00625, >99% purity). Laser particle analyses showed a modal grain size of ~100 μm and that 93% of the grains are finer than 178 μm (Figure 1a). A scanning electron microscope (SEM) image showed that the grains are angular. Na-bentonite powder acquired from Kunimine Industries Co. Ltd (product name: Kunigel) was used to obtain smectite clay. The Na-bentonite powder contained impurities, identified as quartz by X-ray diffraction analysis. Thermogravimetric and differential thermal analysis (TG-DTA, the same analysis as used by *Takahashi et al*. [2007]) revealed that impurities comprise up to 23.5 wt % of the bulk product. Laser particle analyses revealed a bimodal grain size distribution with peaks at ~3.5 and 25 μm and that 90% of the grains are finer than 25 μm (Figure 1b). The quartz and Na-bentonite powders were mixed at gravimetric bentonite contents (fractions) of 5, 7.5, 10, 15, 20, 25, 30, 35, 40, 50, 75, and 100 wt % under room-dry conditions (i.e., 40% relative humidity, two-layer hydration state of smectite), then converted to gravimetric smectite contents of 3.8, 5.7, 7.7, 11.5, 15.3, 19.1, 23.0, 26.8, 30.6, 38.3, 53.6, and 76.5 wt % allowing for the impurity (quartz) in the Na-bentonite powder (hereafter the term "wt %" refers to the content of smectite). Although the ratios of the mixtures should be expressed as a

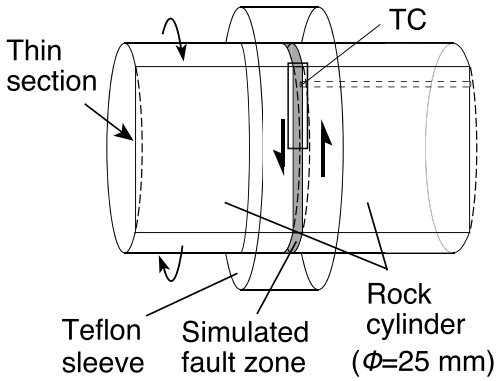

Figure 2. Specimen configuration used in this study. Simulated fault gouge was placed between two cylinders of gabbro or sandstone host rocks. Temperature was measured using a K type thermocouple (TC), placed ~3.5 mm inward from the circumference of the cylinder. The tip of the thermocouple was exposed to a surface between the gouge zone and host rock on the stationary side. Thin sections were made perpendicular to the gouge zone about 4 mm inward from the circumference of the cylinder. The solid box indicates the panoramic images shown in Figure 7. Half arrows show the shear direction.

volumetric content in terms of the packing structure of clasts and matrix in situ, it is difficult to determine the density of swelling clay minerals under water-saturated and pressurized conditions. The simplest and least ambiguous way to express the ratios of the mixtures is as a gravimetric content at a given hydration state. Therefore, our simulated gouge mixtures were designated as gravimetric contents at a two-layer hydration state of smectite.

2.2. Experimental Procedures

One gram samples of simulated fault gouge were saturated with 0.5 ml of distilled water and placed between two cylinders of host rock with diameters of 25.0 mm for all runs (Figure 2). A Teflon sleeve with a 24.95 mm inner diameter was placed around the simulated fault zone to prevent gouge leakage. Initial thicknesses of the gouges were about 1.2, 1.4, and 1.6 mm for pure quartz gouge, 15.3 wt % smectite mixture, and 38.3 wt % smectite mixture, respectively. We used two different types of host rock: gabbro (porosity = 1.6%, permeability = $<10^{-20}$ m^2) in 146 experiments and sandstone (porosity = 15.7%, permeability = 10^{-16} m^2) in 16 experiments to examine the effect of host rock permeability on frictional behavior. The friction experiments were performed using rotary shear, low- to high-velocity friction apparatuses at the Kochi Institute for Core Sample Research, at the Japan Agency for Marine–Earth Science and Technology (JAMSTEC), Kochi, Japan (HVR apparatus [*Hirose and Shimamoto*, 2005] and PHV apparatus [*Tanikawa et al*., 2012a]), and a similar apparatus at the National Institute of Advanced Industrial Science and Technology (AIST), Tsukuba, Japan (HDR apparatus [*Togo and Shimamoto*, 2012]). The experiments were conducted at a normal stress (σ_n) of 2.0 MPa and with equivalent slip rates (V_e) of 30 μm/s to 1.3 m/s, and displacements of 0.5–33 m. Because the slip rate increases from the center to the periphery of the cylindrical specimens, we used the equivalent slip rate, V_e, defined such that $\tau V_e S$ gives the rate of total frictional work on a fault with area S, assuming a constant shear stress, τ, over the fault surface [*Shimamoto and Tsutsumi*, 1994]. For convenience, we refer to "equivalent slip rate" as simply "slip rate" or "velocity (V)." In this study, we defined three ranges of slip rate: low, intermediate, and high, corresponding to 30 μm/s, 150 μm/s to 56 mm/s, and 0.13–1.3 m/s, respectively.

Before each experiment, the specimen was rotated back and forth several times under a lower normal stress of <0.5 MPa to ensure a uniform gouge thickness, then held for 5 min after applying the target normal stress (precompaction treatment). During the precompaction, we found that a small amount of water was squeezed out from between the rock cylinders and Teflon sleeve; hence, we considered the gouge to be saturated with water. For experiments in which the duration exceeded 1 h, we wrapped the specimen in a polyolefin film to prevent drying of the gouge. We conducted two series of experiments at constant normal stress: (1) continuous shearing during a single run and (2) slide-hold-slide tests to examine strength recovery during the holding. We measured the compaction/dilation and temperature of the fault zone during shearing, as well as shear and normal stresses. We placed K type thermocouples on the stationary side of the host rock for five experiments to measure the temperature of the fault zone during shearing (see Figure 2). The tip of the thermocouple was placed close to the area where temperature of the gouge zone becomes maximal as suggested by finite element method modeling [e.g., *Kitajima et al*., 2010; *Han et al*., 2011]. To correct for the effects of friction between the Teflon sleeve and the cylinder, we measured the shear traction in experiments without gouge and then subtracted the traction from the measured raw data of the gouge experiments (for details, see *Oohashi et al*. [2011]).

2.3. Permeability Measurements

The permeability of host rocks and gouges was measured using oil-confined, permeability testing apparatus in JAMSTEC, Kochi [*Tanikawa et al.*, 2010], to investigate the effect of hydrological properties on mechanical behavior. We used unsheared (compacted under $\sigma_n = 2$ MPa) and sheared (compacted and sheared under $\sigma_n = 2$ MPa and $V = 22$ mm/s) mixed gouges with 15.3 wt % and 26.8 wt % smectite between sandstone host rocks to obtain permeability before and after shearing. The permeability of the pure quartz gouge prior to shearing was also measured. We deformed the sheared specimens to achieve 5.46 and 5.61 m displacement for the specimens with 15.3 wt % and 26.8 wt % smectite, respectively. The specimen assembly was taken out from the friction-testing apparatus and then the permeability of the confined gouge layer was measured perpendicular to the layer, following *Tanikawa et al.* [2012b]. After each deformation test, we removed the Teflon sleeve from the specimen assembly without disturbing the gouge zone and then wrapped it with a polyolefin heat-shrink jacket for permeability measurements. We first measured the bulk permeability of the assembly (the gouge layer with two sandstone cylinders) normal to the shear direction then measured the permeability of the host rock sandstone alone. We then estimated the permeability of the gouge layer, k_g, based on the following equation [*Tanikawa et al.*, 2010]:

$$\frac{1}{k_b} = \frac{n}{k_g} + \frac{1-n}{k_s} \tag{1}$$

where k_b is the laboratory-measured bulk permeability, k_s is the permeability of the sandstone cylinders, and n is the ratio of gouge thickness to the total length of the specimen. Measurements were conducted at room temperature (20°C) under confining pressures, P_c, of 2 and 3 MPa, effective pressures, P_e, of 1 and 2 MPa, and values of ΔP_p (upstream pore pressure-downstream pore pressure) of 0.1–0.3 MPa.

3. Results

3.1. Mechanical Behavior During Continuous Shearing Experiments

At a low slip rate of 30 μm/s in gabbro host rock, all mixtures exhibited rapid strengthening within the first 0.5 m of displacement (Figure 3a) then remained at a nearly constant friction coefficient (steady state friction, μ_{ss}) throughout the remainder of the experiment. For a slip rate of 150 μm/s, pure quartz gouges and mixtures with low smectite contents (<19.1 wt %) showed similar behavior to gouges at $V = 30$ μm/s. In contrast, mixtures with ≥23 wt % smectite exhibited low friction values within the first 1 m of displacement, followed by a gradual strengthening, with friction achieving a steady state after more than 1–2 m of displacement. For $V = 1.3$ mm/s, the 7.7–19.1 wt % smectite mixtures exhibited variable behavior, characterized by a gradual strengthening followed by a rapid drop in friction and a fluctuation of >0.2 units in the coefficient of friction. In contrast, the friction coefficients of 26.7 and 38.3 wt % mixtures exhibited slip strengthening in the first ~0.3 m of displacement, followed by slip weakening to a μ_{ss} of ≤0.1. For $V = 22$ mm/s, slip-weakening behavior appeared even for mixtures with relatively low smectite contents (15.3–38.3 wt %), which showed slip strengthening in the first ~0.8 m of displacement, then declined to a very low μ_{ss} of 0.1–0.05. The 7.7 wt % smectite mixtures again showed variable frictional behavior in the slip rates of 22–56 mm/s (Figure 3a). Pure quartz gouge showed neither slip weakening nor variable behavior of friction at slip rates from 1.3 to 22 mm/s. At the highest slip rate of 1.3 m/s, remarkable slip-weakening behavior became apparent even for the 7.7 wt % mixture and for pure quartz gouge, but the level of μ_{ss} had a tendency to decrease with increasing smectite content in the same manner as observed at lower slip rates.

The dependence of the friction coefficient on smectite content varies with both slip rate and displacement (Figure 3b). The relationship between μ_{ss} and the smectite content at $V = 30$ and 150 μm/s shows a marked decrease in friction at moderate smectite contents of 20–50 wt %. The relationship between friction and smectite content shows a close fit to a sigmoidal curve described by the following empirical equation [*Oohashi et al.*, 2013]:

$$\mu = \mu_{100} + (\mu_0 - \mu_{100})/(1 + (x/C_w)^S) \tag{2}$$

where μ, μ_0, and μ_{100} are the coefficients of friction of mixed gouge, pure quartz, and pure smectite, respectively; x is the smectite content (in wt %); C_w is the critical weakening content (the smectite content that reduces the coefficient of friction to half the original), and S is the slope parameter. The fittings give C_w of ~24 wt % for both slip rates of 30 and 150 μm/s. At $V = 1.3$ and 22 mm/s, the friction content curves are

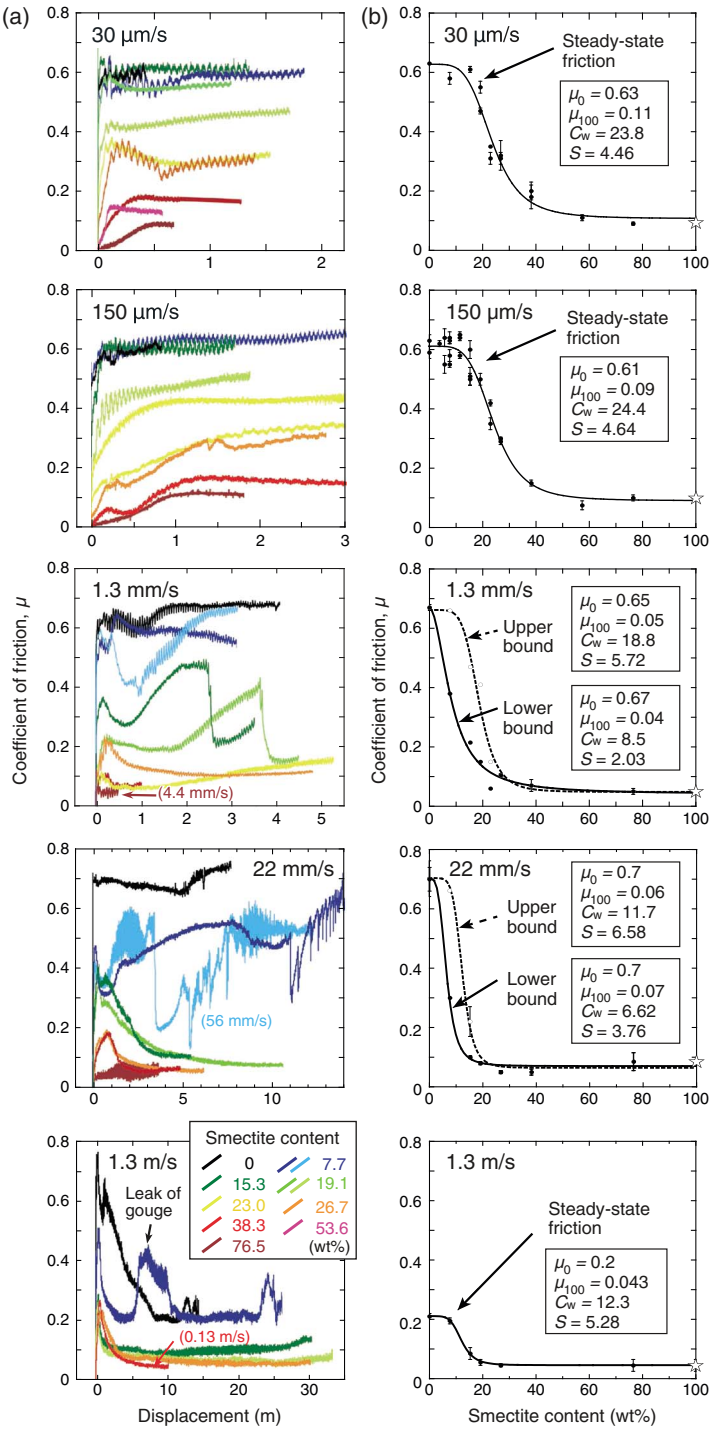

Figure 3. (a) Representative mechanical behaviors of mixed smectite-quartz gouges at slip rates from 30 μm to 1.3 m/s. (b) Steady state friction coefficients as a function of smectite content, for $V = 30$ μm/s, 150 μm/s, and 1.3 m/s. For $V = 1.3$ and 22 mm/s, maximum (open circles) and minimum (filled circles) friction values during variable behaviors of friction are shown as upper and lower bounds, because steady state values are difficult to define. Cylinders of gabbro (host rock) were used for all experiments. The curves in Figure 3b show the least squares fit to each data set using equation (2). We used Kaleidagraph software for the fitting. The fit parameters are shown in each diagram. Differences in frictional strength between gouges with the same smectite content are possibly due to slight heterogeneity of the starting material in the gouge zone and/or the tightness of the Teflon sleeve. The parameter C_w is a threshold value at which weak phase (smectite) starts to govern the strength of the fault zone. The parameter S indicates how rapidly the strength drops with increasing smectite content in the friction–content diagram.

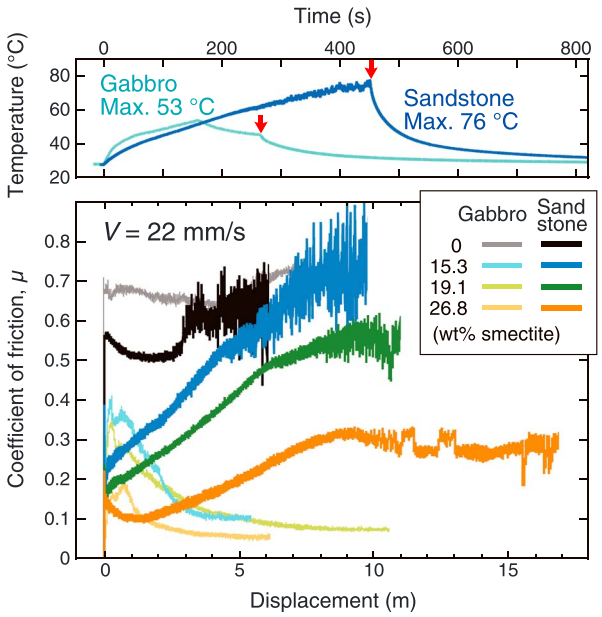

Figure 4. Comparison of the frictional behavior and slip zone temperature of experiments at $V = 22$ mm/s, using gabbro and sandstone host rocks. The temperature of a sliding surface was measured for mixed gouges with 15.3 wt % smectite and using both gabbro and sandstone host rocks. The red arrow indicates the cessation of slip.

expressed with upper and lower bounds of friction level in friction displacement curves in Figure 3b. Both bounding curves show a sudden fall to the same friction level as pure smectite at a smectite content of only 10–30 wt %, as compared with those for $V = 30$ and 150 μm/s. The fittings give C_w of 18.8 wt % (upper bound) and 8.5 wt % (lower bound) for $V = 1.3$ mm, and 11.7 wt % (upper bound) and 4.88 wt % (lower bound) for $V = 22$ mm. At the highest slip rate of 1.3 m/s, the fitting for steady state friction coefficients gives C_w of 12.3 wt %.

The mechanical behavior of mixtures sheared with sandstone host rocks at $V = 22$ mm/s is different from the case of gabbro host rocks (Figure 4). For sandstone host rocks, low friction at the onset of slip gradually increased with displacement and then reached a near steady state with a higher friction level than for the case with gabbro host rocks. The steady state friction coefficients are similar to those at $V = 30$ μm/s and with gabbro host rocks (compare Figures 4 and 3a). The bulk temperature of the sliding surface at steady state friction reached ~53°C for gabbro host rocks and ~76°C for sandstone host rocks (Figure 4).

3.2. Mechanical Behavior During Slide-Hold-Slide Tests

To examine the processes of dynamic weakening at intermediate velocities, slide-hold-slide tests were conducted on 15.3 wt % smectite mixtures. In the tests we suspended the sliding for various durations once the steady state friction ($\mu_{ss,\ 1st}$) had been attained at $V = 22$ mm/s (first run) and then allowed sliding again at $V = 150$ μm/s where dynamic weakening does not occur (second run), to determine if and how the frictional strength recovers during the hold time. The results show that the friction coefficient instantaneously recovered to a certain level (initial friction coefficient of second run, $\mu_{i\ 2nd}$; see Figure 5a) immediately after the onset of the second run. The bulk temperature of the sliding surface, which was elevated to 40–45°C during the first run, rapidly decreased to room temperature during holding for 104 s and in the early stages of the second run (yellow line in Figure 5a). We defined the strength recovery during holding by using $\Delta\mu = (\mu_{i,\ 2nd} - \mu_{ss,\ 1st})$. A plot of $\mu_{i,\ 2nd}$ and $\Delta\mu$ obtained from nine individual tests increases logarithmically during the hold time toward a level of μ_{ss} obtained from continuous shearing experiments at $V = 150$ μm/s, and finally, the strength recovery was almost complete at a hold time of ~10^4 s (Figures 5b and 6). Although the temperature of the sliding surface also decayed logarithmically with time during holding (Figure 6), it settled to room temperature at ~5×10^2–10^3 s after sliding, which was ~1×10^4 s earlier than the time taken for complete strength recovery.

3.3. Permeability of the Fault Zones

The permeability of the gouge zones was obtained for mixed gouges with 15.3 and 26.8 wt % smectite both before and after the shearing under $\sigma_n = 2$ MPa and $V = 22$ mm/s, to assess the effect of permeability on dynamic weakening at intermediate velocities. The permeability of unsheared pure quartz gouge was also measured for comparison. The results show that permeability of unsheared gouge (under $P_c = 2$ MPa) drastically decreased from 6.32×10^{-14} through 6.8×10^{-18} to 2.46×10^{-19} m^2 as the smectite content

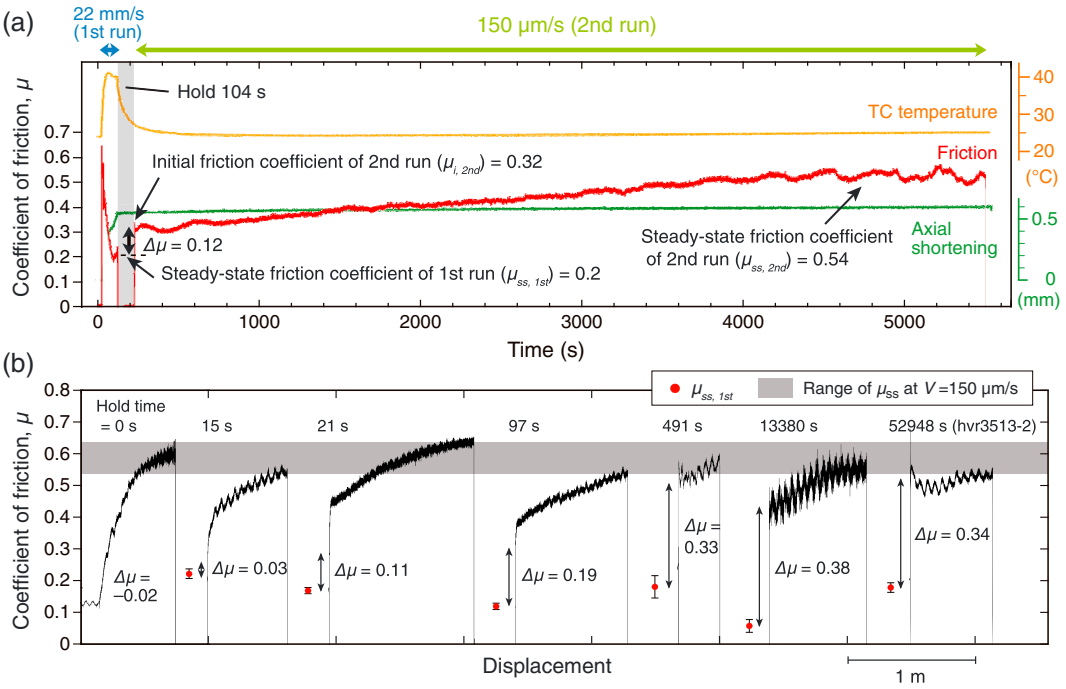

Figure 5. Results of slide-hold-slide tests conducted for mixed gouges with 15.3 wt % smectite at $\sigma_n = 2$ MPa. (a) Representative behavior of the friction coefficient, axial displacement, and slip zone temperature during the slide-hold-slide test. We suspended the sliding for 104 s after steady state had been attained at $V = 22$ mm/s (steady state friction coefficient of first run, $\mu_{ss,\ 1st} = 0.2$), then allowed sliding again at $V = 150$ μm/s where dynamic weakening does not occur. The coefficient of friction instantaneously recovered to ~0.32 (initial friction coefficient of second run, $\mu_{i,\ 2nd}$) after the holding, then increased gradually to 0.54, which corresponds to μ_{ss} for a 15.3 wt % mixture, as obtained from a continuous shearing experiment. We defined the strength recovery during the hold period by using $\Delta\mu = (\mu_{i,\ 2nd} - \mu_{ss,\ 1st})$. Temperature was measured using a K type thermocouple, the tip of which was exposed to the sliding surface of the host rock cylinder. (b) Coefficient of friction plotted against slip displacement for the second runs with hold times of 0–52,948 s. Each friction displacement curve represents an individual experiment. Although $\mu_{ss,\ 1st}$ varies in the experiments (0.05–0.22), $\Delta\mu$ increases logarithmically with holding time. The shaded area shows the range of μ_{ss} for a mixture with 15.3 wt % smectite at $V = 150$ μm/s, as obtained from continuous shearing experiments. Normal stress to the simulated fault was kept constant during the hold period for all runs. Note that a slight kickback (reverse rotation) of the servo-controlled motor at the cessation of the first run acted to remove shear stress during the hold period.

increased from 0 wt % through 15.3 wt % to 26.8 wt % (Table 1). The permeability of the 15.3 wt % and 26.8 wt % mixtures was further reduced by 44% and 25%, respectively, when they were sheared.

4. Fault Zone Microstructures

Fault zone microstructures in three mixed gouges with 15.3 wt % smectite that showed different frictional behavior were analyzed using optical and scanning electron microscopes, to investigate the influence of texture on dynamic weakening at intermediate velocities. The three gouges were from (1) an experiment with gabbro host rocks that showed high μ_{ss} at $V = 30$ μm/s, (2) an experiment with gabbro host rocks that showed slip-weakening behavior and low μ_{ss} at $V = 22$ mm/s (see Figure 3a), and (3) an experiment with sandstone host rocks that showed slip-strengthening behavior and high μ_{ss} at $V = 22$ mm/s (see Figure 4).

The gouge zone with gabbro host rocks sheared at $V = 30$ μm/s has a homogeneous shearing texture with randomly distributed quartz grains of 20–100 μm in diameter and a matrix of finely comminuted quartz clasts (less than a few micrometers in grain size) and smectite particles (Figures 7a and 7b). Shear deformation textures, such as composite planar fabrics, are not observed within the zone. Detailed microscopic observations at the boundaries between the host rocks and the gouge zone, as well as within the gouge zone, show no visible localized slip zones or foliation defined by oriented clay particles (Figures 7c and 7d). The gouge zone with gabbro host rocks sheared at $V = 22$ mm/s also shows the same homogeneous, random shearing texture as that seen for $V = 30$ μm/s (Figures 7e–7g). Roughly 10 large grains of quartz (few tens to 100 μm in diameter)

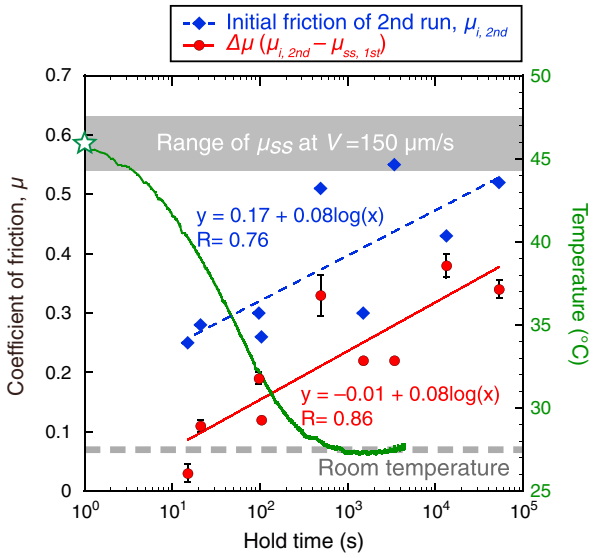

Figure 6. Initial friction coefficients of the second run ($\mu_{i,\ 2nd}$) and strength recovery ($\Delta\mu$) obtained from slide-hold-slide tests plotted against hold time with a logarithmic scale. The shaded area shows the range of μ_{ss} for a mixture with 15.3 wt % smectite at V = 150 μm/s obtained from continuous shearing experiments. The green curve is a representative temperature profile of a sliding surface during the hold period. The star denotes the maximum temperature achieved during the first run. Note that a negative $\Delta\mu$ (−0.02) observed from the hold period of 0 s (see Figure 5b) is not shown in the diagram.

can be recognized perpendicular to the gouge zone, and these quartz grains are usually in contact with each other (red arrows in Figure 7h). The gouge zone with sandstone host rocks sheared at V = 22 mm/s shows similar textures (Figures 7i–7l). The higher proportion of fine matrix (Figure 7j) compared with the case with gabbro host rocks may be attributable to the greater displacement (d = 10.35 m). In addition, the rough surfaces of the sandstone cylinders (compare Figures 7e and 7i) might have enhanced the comminution of grains as proposed by *Niemeijer et al.* [2010]. However, it should be noted that the gouge zones in runs with both gabbro and sandstone host rocks show a random and homogeneous deformation fabric, even though their mechanical behavior is quite different (Figure 4).

5. Discussion and Implications

5.1. Dynamic Weakening at Intermediate Slip Rates

The dramatic slip weakening of smectite-quartz mixtures observed at a slip rate of ~10^{-2} m/s occurs at a slip rate of 1 to 2 orders of magnitude lower than that observed in previous experiments with various types of rocks and gouges (10^{-1} to 10^{0} m/s) [*Di Toro et al.*, 2011]. The increases in bulk temperature in the gouge zone during weakening (to 40–50°C, Figures 4, 5a, and 6) were insufficient to induce dynamic weakening mechanisms, such as thermal decomposition and frictional melting, at coseismic slip rates [see *Di Toro et al.*, 2011]. In addition, a gouge zone with sandstone host rocks attained a higher temperature than that with gabbro host rocks. Thus, the weakness of mixed gouges at intermediate slip rates and with gabbro host rocks was not simply caused by frictional heating. Weakening due to silica gel formation [*Goldsby and Tullis*, 2002] can also be ruled out because pure quartz gouge does not show such weakening. Numerous studies have shown fabric development to be an effective weakening mechanism at low slip rates [e.g., *Bos and Spiers*, 2001; *Collettini et al.*, 2009; *Oohashi et al.*, 2013]. However, fabrics such as an interconnected weak mineral network or through-going slip surfaces (e.g., see *Collettini et al.* [2009, Figure 4a] and *Oohashi et al.* [2013, Figure 8]) could not be recognized from the experiments, indicating low μ_{ss} at an intermediate slip rate

Table 1. Summary of Permeability Measurements[a]

	Gouge Permeability (m^2) at ΔP_p = 0.2 MPa				
	Preshear		Sheared (V = 22 mm/s)		
Smectite Fraction	P_c (MPa) = 2	3	P_c (MPa) = 2	3	Shear displacement
0 wt %	6.32E−14	4.63E−14	–	–	–
15.3 wt %	6.80E−18	1.62E−18	2.99E−18	7.78E−19	5.46 m
26.8 wt %	2.46E−19	1.19E−19	6.07E−20	3.55E−20	5.61 m

[a] ΔP_p = (upstream pore pressure − downstream pore pressure).

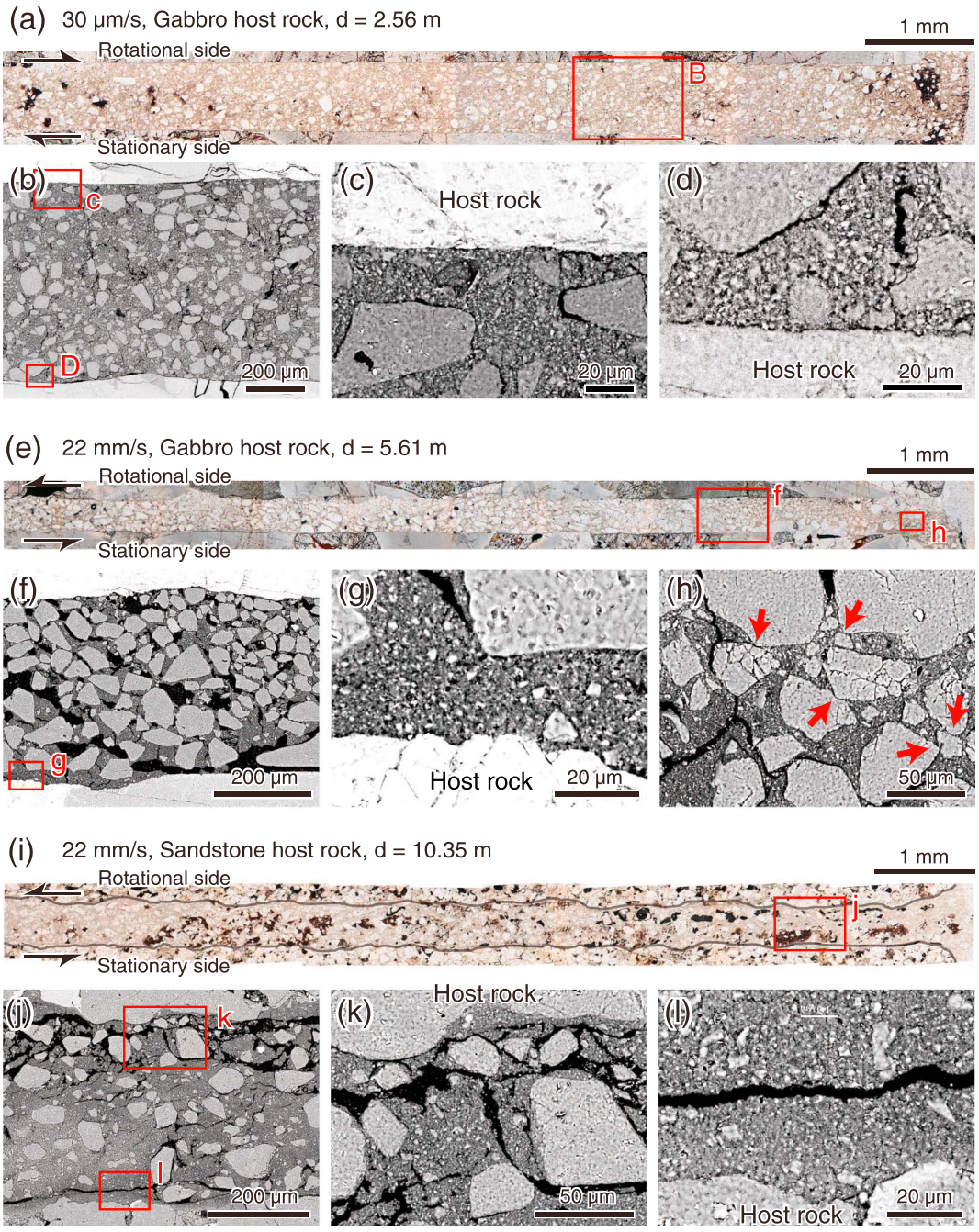

Figure 7. Textures of gouge zones with 15.3 wt % smectite, sheared at (a–d) $V = 30$ μm/s with gabbro host rocks; (e–h) $V = 22$ mm/s, gabbro; and (i–l) $V = 22$ mm/s, sandstone. The first image of each group is a panoramic, plane-polarized light photo; the right end corresponds to the outer edge of the cylinder and half arrows indicate the shear direction. All other images are close-up, backscattered electron SEM photos. Red arrows in Figure 7h show quartz-quartz grain contacts. Solid lines in Figure 7i denote host rock-gouge boundaries.

($V = 22$ mm/s). Therefore, neither thermal decomposition and frictional melting nor fabric-induced weakening is likely to be associated with the weakening at intermediate slip rates. We consider that an increase in pore pressure in the smectite-bearing gouge zone is potentially the cause of the observed weakening, because the permeability of the host rock has a large effect on a pore pressure rise and because the mechanical behavior of a fault zone differs with the host rock.

In the high-velocity friction experiments, pore pressure can be elevated during the shearing in the following ways: dehydration of hydrous minerals and vaporization of pore fluids due to frictional heat, and shear-enhanced compaction [see *Brantut et al*., 2008; *Ujiie et al*., 2011; *Faulkner et al*., 2011]. In this section, we examine the former case. The vaporization of water is considered to occur due to locally elevated temperature within the gouge zone that results from flash heating at sliding asperity contacts between grains, even though the bulk temperature remained below 100°C (see *Hirose and Bystricky* [2007] for the case of serpentine dehydration). The flash temperature at asperity contacts can be estimated as follows:

$$\Delta T = 0.345 \frac{\mu \pi p_m}{\rho C_p} \sqrt{\frac{a V_a}{2\kappa/\rho C_p}} \tag{3}$$

where μ is the coefficient of friction, ρ is density, C_p is the heat capacity, P_m is the compressive yield strength, κ is thermal conductivity, a is the asperity contact radius, and V_a is the sliding velocity at asperity contacts [*Archard*, 1959; *O'Hara*, 2005]. We used the following values to calculate the temperature at quartz-quartz grain contacts: $\rho = 2700$ kg/m^3, $C_p = 760$ J/kg K, $P_m = 8$ GPa [*Masuda et al*., 2000], and $\kappa = 1.38$ W/m K. We estimated $a = 10$ μm based on textural observations (see Figure 7h). For $V = 22$ mm/s, we assumed $V_a = 2$ mm/s, because slip seemed to be distributed within the gouge zone and about 10 large grains of quartz are usually recognized perpendicular to the zone (see Figure 7f, with an assumption of homogeneous strain). The calculated temperature ΔT at $V = 22$ mm/s is 309°C, high enough to vaporize the pore water at a pressure of 2 MPa (boiling temperature = 210°C, calculated using the Antoine equation). Also, the calculated temperature is high enough to cause dehydration of smectite [*Colten-Bradley*, 1987], which may enhance fluid pressure. In contrast, ΔT at $V = 150$ μm/s is suppressed to <84°C (even if we assume $V_a = 150$ μm/s), which cannot lead to vaporization (and significant dehydration of smectite) and resultant weakening.

Friction showed variable behavior for mixtures with 7.7–19.1 wt % smectite sheared at $V = 1.3$ mm/s, and for a mixture with 7.7 wt % smectite sheared at $V = 22$ and 56 mm/s. In cases where friction showed variable behavior, we did not find visible gouge leakage and/or evidence of episodic rotation of the Teflon sleeve, which would cause an irregular change in traction between the host rocks and Teflon sleeve. Although observations of texture during the variable behavior are lacking, the behavior can be considered a "transitional behavior" that occurs between conditions where microscopic thermal pressurization is ineffective and where it becomes effective. V_a of about 1 mm/s is a threshold at which the temperature of asperity contacts becomes equal to boiling temperature under a pressure of 2 MPa. Thus, the variable behavior at $V = 1.3$ mm/s may be caused by episodic activation/deactivation of vaporization due to slight decreases/increases in the width of the active slip zone (temporal slip localization) during shearing, which causes a fluctuation in sliding velocity at the asperity contacts. On the other hand, the behavior observed for a mixture with 7.7 wt % smectite at $V = 22$ and 56 mm/s may be explained by the competing effects of pressurization and diffusion during shearing, due to the high permeability of the gouge.

5.2. Effect of Compaction-Induced Pressurization on Weakness at Intermediate to High Slip Rates

For $V = 150$ μm/s, mixtures with $\geq$23 wt % smectite exhibited low friction values within the first 1 m of displacement, then the friction gradually increased to a steady state through 1–2 m of displacement. Flash heating at a sliding asperity cannot explain this low friction because the estimated temperature is insufficient to vaporize pressurized pore water. In addition, the strength recovery during slide-hold-slide tests at $V = 22$ mm/s occurs over a much longer time than the decay of measured slip zone temperature. This implies that not only frictional heating but also other factors have an effect on weakening at intermediate velocities. Therefore, we examine the effect of compaction-induced pressurization on weakening.

Compaction-induced pressurization is efficient when the compaction (porosity loss) proceeds faster than the diffusion of the pore fluids. The slip rate and displacement at the center of the specimen is zero, so shear-enhanced compaction should be negligible there, but they gradually increase to a maximum approaching the periphery of the gouge zone. The pressurized pore fluids near the periphery of the gouge may be released by either drainage through the gap between the cylinders and the Teflon sleeve or by migration into the center of the gouge, due to the low permeability of the gabbro host rocks. Torque due to the shear stress acting on the outer half of the gouge zone is as large as 87.5% of the total torque produced by shear stress acting on the entire surface, if the shear stress is uniform. Thus, we estimate the time required

for the pressurized fluids in the outer half of the gouge zone to migrate to the center or the periphery of the gouge (a distance of radius/2), to assess the time taken for the outer half of the gouge zone to recover to an unpressurized state.

The characteristic diffusion time, t_D, for the radial flow of pressurized fluids can be estimated as follows:

$$t_D = d^2/D_h \tag{4}$$

where d is the characteristic distance and D_h is hydraulic diffusivity [*Ingebritsen and Sanford*, 1998]. D_h is given by $D_h = k/\varphi\eta(\beta_f + \beta_m)$, where k *is* permeability, φ is porosity, η is the viscosity of pore fluid, and β_f and β_m are the compressibility of pore fluid and matrix, respectively. These relationships define the time, t_D, at which the pressure change at d will be 1/10 of the pressure change at the pressure sink. We assumed the following values to calculate the t_D of pore water: $d = 6.25 \times 10^{-3}$ m (radius/2), $\beta_f = 0.45 \times 10^{-9}$ m^2/N, $\beta_m = 2.1 \times 10^{-6}$ m^2/N (compressibility of soft clay) [*Domenico and Mifflin*, 1965], $\varphi = 0.26$, and $\eta = 1 \times 10^{-3}$ Pa s. Because the permeability of the gouge changes as shearing progresses, we adopted values of k of both the unsheared gouge (1.62×10^{-18} m^2) and the sheared gouge (7.78×10^{-19} m^2) of the mixture with 15.3 wt % smectite (Table 1). The calculated t_D is 1.31–2.75×10^4 s, which is comparable to the duration of compaction, t_C, of about 1×10^4 s at $V = 30$ μm/s (Figure 8a) but longer than t_C of about 1–3×10^3 s at $V = 150$ μm/s (Figure 8b).

These results suggest that the pore pressure rise due to shear-induced compaction was not generated for experiments at $V \leq 30$ μm/s, because the pressurized fluids diffused at almost the same time as compaction occurred. In contrast, for the experiments at $V = 150$ μm/s, rapid compaction, which progressed faster than diffusion, may cause a rise in pore pressure and resultant low frictional strength in the first ~1 m of displacement; subsequent diffusion may promote slip strengthening. Since pressurization may increase when gouge permeability decreases and/or shear compaction progresses rapidly, pressurization may also have contributed to reducing the friction for the experiments using mixtures with >15.3 wt % smectite and at $V > 150$ μm/s (see the shortening curves for higher sliding velocities in Figure 8c). However, this process only occurs if the fault zone possesses high initial porosity that can be lost with slip. In fact, we have confirmed that the low friction in an early stage of sliding was suppressed when we slid the same specimen again (see mechanical behavior and axial shortening of hvr3513-2 in Figures 5b and 8b). The calculated diffusion time also indicates that the strength recovery during slide-hold-slide tests, which were completed after a hold time of about 10^4 s, can be explained by diffusion of elevated pore pressure.

5.3. Effect of Permeability on the Intermediate Velocity Frictional Behavior of Fault Zones

Most of the friction at intermediate to high slip rates reported in this paper is not a material property of the gouge but rather an "apparent friction" as a consequence of fluid overpressure, as numerically demonstrated by *Tanikawa et al*. [2013] in the case of high-velocity sliding. The permeability of the gouge zones shows a rapid decrease with increasing smectite content up to only 20 wt %, and the rate of permeability reduction was more significant when the gouge experienced shearing (Table 1). Our SEM images of these gouges show a densely packed, fine matrix of quartz and smectite, and this may explain the low permeability at low smectite contents. The high permeability of the pure quartz gouge may explain why this gouge did not weaken at intermediate slip rates.

The experiments with sandstone host rocks clearly demonstrated that impermeable surroundings are necessary to bring about weakening at intermediate velocities. In the case of experiments with sandstone host rocks, pressurized fluids are considered to escape into the host rocks by migration perpendicular to the zone, due to the high permeability of the sandstone. The calculated t_D for this configuration (using $d = 0.5 \times 10^{-3}$ m, gouge thickness/2, and $k = 1.62 \times 10^{-18}$ to 7.78×10^{-19} m^2) is 84–176 s, rapid enough to diffuse the elevated pressure (and thus produce slip-strengthening behavior) during the experiment. Those results imply that we have to be careful about the effect of pore pressure when we measure the intrinsic frictional properties of such an impermeable material even under several tens or hundreds of μm/s. Overall, we conclude that the abrupt strength reduction observed for mixtures with ≥15.3 wt % smectite at intermediate velocities and with gabbro host rocks was caused by microscopic thermal pressurization and compaction-induced pressurization assisted by the low permeability of the gouge and host rocks. Those weakening processes at intermediate velocities may also be important for impermeable natural fault gouge, such as clay-rich and/or extremely fine-grained fault gouge.

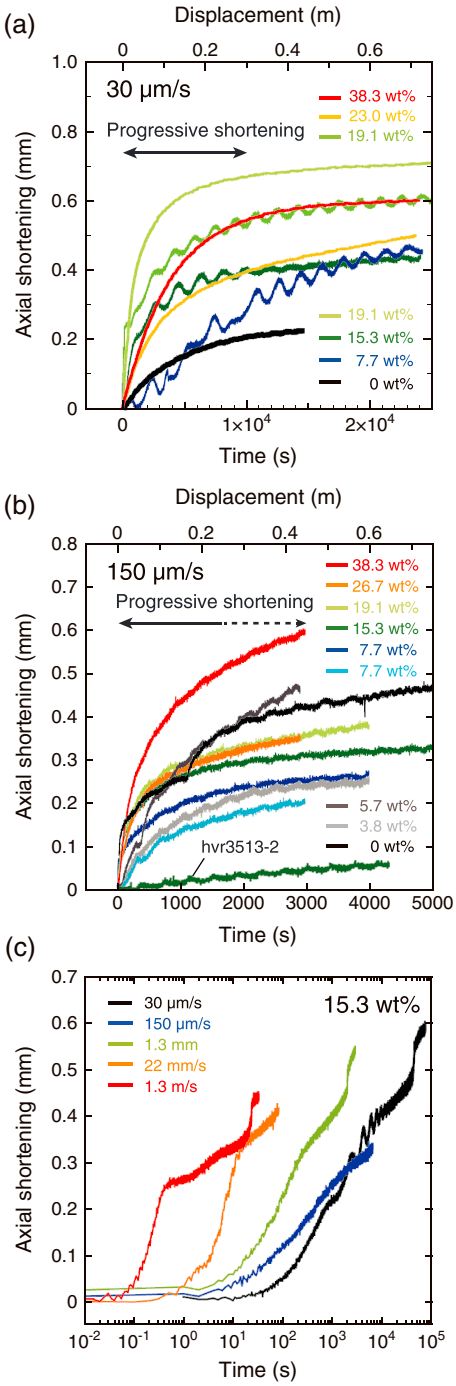

Figure 8. Axial shortening of the mixed gouge layer plotted against time (and slip displacement) for the experiments at (a) $V = 30$ μm/s and (b) $V = 150$ μm/s. The term "wt %" in the figure refers to the content of smectite. Progressive shortening, mainly due to shear-induced compaction, was observed in the first 10,000 s and 1000–3000 s of the experiments at $V = 30$ and 150 μm/s, respectively, although we observed large shortening, probably due to leakage of the gouge, in several experiments. The hvr3513-2 (see Figure 5b, a slide-hold-slide test with the longest hold time of about 53,000 s) was sheared at $V = 150$ μm/s after the first run of about 2.6 m in displacement. (c) Axial shortening of the mixed gouge layer with 15.3 wt % smectite plotted against time for the experiments at $V = 30$ μm/s to 1.3 m/s (logarithmic scale).

5.4. Implications for Subduction Zone Earthquakes

Although seismic slip is basically a pulse-like rupture with various rates of acceleration and deceleration, our results of constant slip rate experiments may have important implications for understanding the frictional responses of the shallow plate interface to updip rupture propagation. During interseismic periods, faults poor in smectite (roughly <30 wt %) (e.g., the megasplay fault in the Nankai Trough; [*Guo and Underwood*, 2012]) may have high friction values of $\mu = 0.5$–0.6 under low slip rates, whereas smectite-rich faults (>30 wt %) developed in hemipelagic sediments (e.g., the décollement in the Nankai Trough; [*Underwood and Guo*, 2013]) have lower values of $\mu < 0.3$ (see Figure 9). At an early stage of seismic sliding, faults with relatively low smectite content (15–30 wt %) likely lose strength abruptly at intermediate velocities of mm/s to cm/s due to microscopic thermal pressurization plus compaction-induced pressurization. This characteristic accelerates a fault slip in response to rupture propagation and potentially facilitates large coseismic slip and stress drop (red arrow in Figure 9). Impermeable surroundings are needed for fault weakening to operate, and the permeability of marine sediments is usually as low as the gabbro used in our experiments [*Gamage et al.*, 2011]. Faults with >50 wt % smectite content have been found in pelagic claystone on incoming oceanic plates (e.g., the décollement in the Japan Trench; [*Kameda et al.*, 2014]). In such a fault, small but perceptible stress drops will be expected to occur (blue arrow in Figure 9) during an earthquake owing to the weaknesses at low slip rates and the velocity-weakening characteristics at intermediate to high slip rates (Figure 3a).

To activate weakening at intermediate slip rates, faults need to slip ~1 m beyond the slip-strengthening stage (see Figure 3a; slip-strengthening behavior in first 0.3–0.8 m displacement at $V = 1.3$ and 22 mm/s) and that strengthening is expected to represent a barrier to rupture propagation. This property possibly leads to slow slip (less than mm/s) if a fault motion does not overcome the barrier. On the other hand, if a fault can

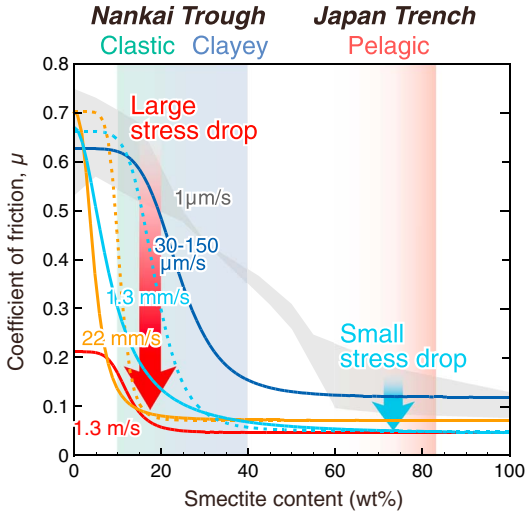

Figure 9. Compilation of the steady state coefficient of friction versus smectite content at slip rates ranging from 1 μm/s to 1.3 m/s. The dotted and solid lines are least squares fits to the experimental data (see the caption to Figure 3b). The friction content curve for 1 μm/s (gray shaded area) is from previous studies [*Logan and Rauenzahn*, 1987; *Takahashi et al.*, 2007; *Tembe et al.*, 2010]. The colored areas show the smectite content of incoming sediments in the Nankai Trough and the Japan Trench.

overcome the barrier by slip, large coseismic slip may propagate updip along a plate boundary fault toward a trench, like the 2011 Tohoku earthquake.

Smectite is more abundant in the southeastern Pacific than in the northwestern Pacific [*Griffin et al.*, 1968] and is more abundant in the northwestern Pacific than in the Shikoku Basin [*Aoki et al.*, 2001]. The spatial heterogeneity of smectite content in sediments may be responsible for differences in seismicity or rupture mode between the Peru-Chile Trench, the Japan Trench, and the Nankai Trough.

6. Conclusions

1. We investigated the frictional properties of water-saturated smectite-quartz mixtures at slip rates from 30 μm/s to 1.3 m/s and with gabbro or sandstone host rocks. At low slip rates of 30 μm/s and gabbro host rocks, the mixtures exhibited rapid strengthening within the first 0.5 m of displacement, then attained a steady state friction. The relationship between steady state friction coefficient and smectite content can be fitted to a sigmoidal curve, and it decreased gradually from 0.5–0.6 to 0.1 with increasing smectite content (from 20 to 50 wt %). At slip rates higher than 1.3 mm/s, friction exhibits marked slip weakening, resulting in low friction coefficients of 0.1–0.05 even for low smectite contents (roughly $<$30 wt %). Thus, the relationship between steady state friction and smectite content suddenly falls to the friction level of pure smectite at a smectite content of only 10–30 wt %. Drastic slip weakening at smectite contents of 10–30 wt % occurs at slip rates of ~10 mm/s, which is 1 to 2 orders of magnitude less than that at which slip weakening was observed in previous experiments on various rock types.
2. In contrast, for the experiments with sandstone host rocks, friction at intermediate velocity shows a completely different behavior: gradually increasing with displacement and then reaching higher steady state friction coefficients than experiments with gabbro host rocks. The permeability of the gouge zones showed a rapid decrease with increasing smectite content up to only 20 wt %, and the reduction in the rate of permeability was more significant when the gouge experienced shearing. Estimates of both flash heating at asperity contacts and the diffusion time of elevated pore pressure suggest that weakening was caused by a rise in pore pressure due to shear-enhanced compaction and microscopic thermal pressurization of pore fluids assisted by the (shear-induced) low permeability of the gouge and host rocks.
3. For the experiments that exhibited high μ_{ss} at low slip rates with gabbro host rocks, low μ_{ss} at intermediate slip rates with gabbro host rocks, and high μ_{ss} at intermediate slip rates with sandstone host rocks, fault zone microstructures did not show clear differences in fabric development. Thus, the weakness of mixed smectite-quartz gouges at intermediate slip rates and with gabbro host rocks was not primarily caused by the development of a fabric such as a foliated network of clay particles.
4. Marine sediments along subduction zones usually contain variable amounts of smectite. Based on our experiments, a fault zone lacking smectite (0–10 wt %) only shows dynamic weakening when the slip velocity attains a seismic slip rate of m/s. On the other hand, a fault zone with a relatively low smectite content (15–30 wt %) likely loses strength abruptly at intermediate velocities in response to rupture propagation from seismogenic depths, leading to an acceleration in fault motion, which potentially facilitates both large coseismic slip and a stress drop near the trench. For a fault zone with abundant smectite ($>$50 wt %), small stress drops are expected to occur during an earthquake owing to the static weakness and the velocity-weakening characteristics at intermediate to high slip rates.

5. Our results clearly indicate that the amount of smectite, and related hydrological properties of fault zones, significantly affects slip behavior at below seismic, subseismic, and seismic slip rates. The wide diversity of frictional behavior among the mixtures with different smectite contents emphasizes the importance of a better understanding of the mineral assemblages of incoming sediments and their spatial distributions along subduction thrust faults.

Acknowledgments

We thank Kyuichi Kanagawa, Masaya Suzuki, Osamu Tadai, and Hiroko Kitajima for constructive discussions and technical help. We sincerely thank André Niemeijer, Dan Faulkner, Diane Moore, Robert Holdsworth, and an anonymous reviewer for careful and constructive reviews and comments on an earlier version of this paper. This work was supported by a JSPS Grant-in-Aid for JSPS fellows (25-04960) to K.O., a JSPS Grant-in-Aid for Scientific Research (25287135) to T.H., and MEXT KANAME grant 21107004. All experimental raw data used in this study are archived at the Kochi Institute for Core Sample Research, at the Japan Agency for Marine–Earth Science and Technology (contact hiroset@jamstec.go.jp) and at the National Institute of Advanced Industrial Science and Technology (contact miki.takahashi@aist.go.jp).

References

Andrews, D. J. (2002), A fault constitutive relation accounting for thermal pressurization of pore fluid, *J. Geophys. Res.*, *107*(B12), 2363, doi:10.1029/2002JB001942.

Aoki, S., N. Kohyama, and K. Oinuma (2001), Clay mineral distribution in surface sediments in the seas and ocean along the eastern Asian continent, with special reference to the relation to morphology and chemistry, *Clay Sci.*, *11*, 431–449.

Archard, J. F. (1959), The temperature of rubbing surfaces, *Wear*, *2*, 438–455, doi:10.1016/0043-1648(59)90159-0.

Bos, B., and C. J. Spiers (2001), Experimental investigation into the microstructural and mechanical evolution of phyllosilicate-bearing fault rock under conditions favouring pressure solution, *J. Struct. Geol.*, *23*, 1187–1202, doi:10.1016/S0191-8141(00)00184-X.

Brantut, N., A. Schubnel, J.-N. Rouzaud, F. Brunet, and T. Shimamoto (2008), High-velocity frictional properties of a clay-bearing fault gouge and implications for earthquake mechanics, *J. Geophys. Res.*, *113*, B10401, doi:10.1029/2007JB005551.

Brown, K. M., A. Kopf, M. B. Underwood, and J. L. Weinberger (2003), Compositional and fluid pressure controls on the state of stress on the Nankai subduction thrust: A weak plate boundary, *Earth Planet. Sci. Lett.*, *214*, 589–603, doi:10.1016/S0012-821X(03)00388-1.

Cole, T. G., and H. F. Shaw (1983), The nature and origin of authigenic smectites in some Recent marine sediments, *Clay Miner.*, *18*, 239–252, doi:10.1180/claymin.1983.018.3.02.

Collettini, C., A. Niemeijer, C. Viti, and C. Marone (2009), Fault zone fabric and fault weakness, *Nature*, *462*, 907–911, doi:10.1038/nature08585.

Colten-Bradley, V. A. (1987), Role of pressure in smectite dehydration—Effects on geopressure and smectite-to-illite transformation, *Am. Assoc. Pet. Geol. Bull.*, *71*, 1414–1427.

Cummins, P. R., and Y. Kaneda (2000), Possible splay fault slip during the 1946 Nankai earthquake, *Geophys. Res. Lett.*, *27*, 2725–2728, doi:10.1029/1999GL011139.

Di Toro, G., R. Han, T. Hirose, N. De Paola, S. Nielsen, K. Mizoguchi, F. Ferri, M. Cocco, and T. Shimamoto (2011), Fault lubrication during earthquakes, *Nature*, *471*, 494–498, doi:10.1038/nature09838.

Domenico, P. A., and M. D. Mifflin (1965), Water from low-permeability sediments and land subsidence, *Water Resour. Res.*, *1*, 563–576, doi:10.1029/WR001i004p00563.

Faulkner, D. R., T. M. Mitchell, J. Behnsen, T. Hirose, and T. Shimamoto (2011), Stuck in the mud? Earthquake nucleation and propagation through accretionary forearcs, *Geophys. Res. Lett.*, *38*, L18303, doi:10.1029/2011GL048552.

French, M. E., H. Kitajima, J. S. Chester, F. M. Chester, and T. Hirose (2014), Displacement and dynamic weakening processes in smectite-rich gouge from the Central Deforming Zone of the San Andreas Fault, *J. Geophys. Res. Solid Earth*, *119*, 1777–1802, doi:10.1002/2013JB010757.

Fujiwara, T., S. Kodaira, T. No, Y. Kaiho, N. Takahashi, and Y. Kaneda (2011), The 2011 Tohoku-Oki earthquake: Displacement reaching the trench axis, *Science*, *334*, 1240, doi:10.1126/science.1211554.

Gamage, K., E. Screaton, B. Bekins, and I. Aiello (2011), Permeability–porosity relationships of subduction zone sediments, *Mar. Geol.*, *279*, 19–36, doi:10.1016/j.margeo.2010.10.010.

Goldsby, D. L., and T. E. Tullis (2002), Low frictional strength of quartz rocks at subseismic slip rates, *Geophys. Res. Lett.*, *29*(17), 1844, doi:10.1029/2002GL015240.

Griffin, J. J., H. Windom, and E. D. Goldberg (1968), The distribution of clay minerals in the world ocean, *Deep Sea Res.*, *15*, 433–459, doi:10.1016/0011-7471(68)90051-X.

Guo, J., and M. B. Underwood (2012), Data report: Clay mineral assemblages from the Nankai Trough accretionary prism and the Kumano Basin, IODP Expeditions 315 and 316, NanTroSEIZE Stage 1, in *Proceedings of the Integrated Ocean Drilling Program*, vol. 314/315/316, edited by M. Kinoshita et al., IODP Management International, Inc., Washington, D. C., doi:10.2204/iodp.proc.314315316.202.2012.

Han, R., T. Shimamoto, T. Hirose, J.-H. Ree, and J. Ando (2007), Ultralow friction of carbonate faults caused by thermal decomposition, *Science*, *316*, 878–881, doi:10.1126/science.1139763.

Han, R., T. Hirose, T. Shimamoto, Y. Lee, and J. Ando (2011), Granular nanoparticles lubricate faults during seismic slip, *Geology*, *39*, 599–602, doi:10.1130/G31842.1.

Hirose, T., and M. Bystricky (2007), Extreme dynamic weakening of faults during dehydration by coseismic shear heating, *Geophys. Res. Lett.*, *34*, L14311, doi:10.1029/2007GL030049.

Hirose, T., and T. Shimamoto (2005), Growth of molten zone as a mechanism of slip weakening of simulated faults in gabbro during frictional melting, *J. Geophys. Res.*, *110*, B05202, doi:10.1029/2004JB003207.

Hyndman, R. D., M. Yamano, and D. A. Oleskevich (1997), The seismogenic zone of subduction thrust faults, *Isl. Arc*, *6*, 244–260, doi:10.1111/j.1440-1738.1997.tb00175.x.

Ingebritsen, S. E., and W. E. Sanford (1998), *Groundwater in Geologic Processes*, 341 pp., Cambridge Univ. Press, New York.

Kameda, J., M. Shimizu, K. Ujiie, T. Hirose, M. Ikari, J. Mori, K. Oohashi, and G. Kimura (2014), Pelagic smectite as an important factor in tsunamigenic slip along the Japan Trench, *Geology*, *43*, 155–158.

Kenney, T. C. (1967), The influence of mineral composition on the residual strength of natural soils, in *Proceedings of the Geotechnical Conference on Shear Strength Properties of Natural Soils and Rocks*, pp. 123–129, Norwegian Geotechnical Institute, Oslo, Norway.

Kitajima, H., J. S. Chester, F. M. Chester, and T. Shimamoto (2010), High-speed friction of disaggregated ultracataclasite in rotary shear: Characterization of frictional heating, mechanical behavior, and microstructure evolution, *J. Geophys. Res.*, *115*, B08408, doi:10.1029/2009JB007038.

Kozdon, J. E., and E. M. Dunham (2013), Rupture to the trench: Dynamic rupture simulations of the 11 March 2011 Tohoku earthquake, *Bull. Seismol. Soc. Am.*, *103*(2B), 1275–1289, doi:10.1785/0120120136.

Logan, J. M., and K. A. Rauenzahn (1987), Frictional dependence of gouge mixtures of quartz and montmorillonite on velocity, composition and fabric, *Tectonophysics*, *144*, 87–108, doi:10.1016/0040-1951(87)90010-2.

Masuda, T., T. Hiraga, H. Ikei, H. Kanda, Y. Kugimiya, and M. Akizuki (2000), Plastic deformation of quartz at room temperature: A Vickers nano-indentation test, *Geophys. Res. Lett.*, *27*, 2773–2776, doi:10.1029/1999GL008460.

Niemeijer, A., C. Marone, and D. Elsworth (2010), Frictional strength and strain weakening in simulated fault gouge: Competition between geometrical weakening and chemical strengthening, *J. Geophys. Res.*, *115*, B10207, doi:10.1029/2009JB000838.
O'Hara, K. (2005), Evaluation of asperity-scale temperature effects during seismic slip, *J. Struct. Geol.*, *27*, 1892–1898, doi:10.1016/j.jsg.2005.04.013.
Oinuma, K., and K. Kobayashi (1966), Quantitative study of clay minerals in some recent marine sediments and sedimentary rocks from Japan, in *Proceedings of the 14th National Conference on Clays and Clay Minerals*, pp. 209–219, Pergamon Press, London.
Oohashi, K., T. Hirose, and T. Shimamoto (2011), Shear-induced graphitization of carbonaceous materials during seismic fault motion: Experiments and possible implications for fault mechanics, *J. Struct. Geol.*, *33*, 1122–1134, doi:10.1016/j.jsg.2011.01.007.
Oohashi, K., T. Hirose, and T. Shimamoto (2013), Graphite as a lubricating agent in fault zones: An insight from low- to high-velocity friction experiments on a mixed graphite-quartz gouge, *J. Geophys. Res. Solid Earth*, *118*, 2067–2084, doi:10.1002/jgrb.50175.
Park, J.-O., H. Naruse, and N. L. Bangs (2014), Along-strike variations in the Nankai shallow décollement properties and their implications for tsunami earthquake generation, *Geophys. Res. Lett.*, *41*, 7057–7064, doi:10.1002/2014GL061096.
Rice, J. R. (2006), Heating and weakening of faults during earthquake slip, *J. Geophys. Res.*, *111*, B05311, doi:10.1029/2005JB004006.
Saffer, D. M., and C. Marone (2003), Comparison of smectite- and illite-rich gouge frictional properties: Application to the updip limit of the seismogenic zone along subduction megathrusts, *Earth Planet. Sci. Lett.*, *215*, 219–235, doi:10.1016/S0012-821X(03)00424-2.
Sakaguchi, A., et al. (2011), Seismic slip propagation to the up-dip end of plate boundary subduction interface faults: Vitrinite reflectance geothermometry on Integrated Ocean Drilling Program NanTroSEIZE cores, *Geology*, *39*, 395–399, doi:10.1130/G31642.1.
Shimamoto, T., and A. Tsutsumi (1994), A new rotary-shear high-velocity friction testing machine: Its basic design and scope of research [in Japanese with English abstract], *Struct. Geol.*, *39*, 65–78.
Summers, R., and J. Byerlee (1977), A note on the effect of fault gouge composition on the stability of frictional sliding, *Int. J. Rock Mech. Min. Sci.*, *14*, 155–160.
Takahashi, M., K. Mizoguchi, K. Kitamura, and K. Masuda (2007), Effects of clay content on the frictional strength and fluid transport property of faults, *J. Geophys. Res.*, *112*, B08206, doi:10.1029/2006JB004678.
Tanikawa, W., M. Sakaguchi, O. Tadai, and T. Hirose (2010), Influence of fault slip rate on shear-induced permeability, *J. Geophys. Res.*, *115*, B07412, doi:10.1029/2009JB007013.
Tanikawa, W., H. Mukoyoshi, and O. Tadai (2012a), Experimental investigation of the influence of slip velocity and temperature on permeability during and after high-velocity fault slip, *J. Struct. Geol.*, *38*, 90–101, doi:10.1016/j.jsg.2011.08.013.
Tanikawa, W., H. Mukoyoshi, O. Tadai, T. Hirose, A. Tsutsumi, and W. Lin (2012b), Velocity dependence of shear-induced permeability associated with frictional behavior in fault zones of the Nankai subduction zone, *J. Geophys. Res.*, *117*, B05405, doi:10.1029/2011JB008956.
Tanikawa, W., H. Takehiro, H. Mukoyoshi, O. Tadai, and W. Lin (2013), Fluid transport properties in sediments and their role in large slip near the surface of the plate boundary fault in the Japan Trench, *Earth Planet. Sci. Lett.*, *382*, 150–160, doi:10.1016/j.epsl.2013.08.052.
Tembe, S., D. A. Lockner, and T.-F. Wong (2010), Effect of clay content and mineralogy on frictional sliding behavior of simulated gouges: Binary and ternary mixtures of quartz, illite, and montmorillonite, *J. Geophys. Res.*, *115*, B03416, doi:10.1029/2009JB006383.
Togo, T., and T. Shimamoto (2012), Energy partition for grain crushing in quartz gouge during subseismic to seismic fault motion: An experimental study, *J. Struct. Geol.*, *38*, 139–155, doi:10.1016/j.jsg.2011.12.014.
Ujiie, K., A. Tsutsumi, and J. Kameda (2011), Reproduction of thermal pressurization and fluidization of clay-rich fault gouges by high-velocity friction experiments and implications in seismic slip in natural faults, *Geol. Soc. Spec. Publ.*, *359*, 267–285, doi:10.1144/SP359.15.
Underwood, M. B., and J. Guo (2013), Data report: Clay mineral assemblages in the Shikoku Basin, NanTroSEIZE subduction inputs, IODP Sites C0011 and C0012, in *Proceedings of the Integrated Ocean Drilling Program*, vol. 322, edited by S. Saito et al., IODP Management International, Inc., Tokyo, doi:10.2204/iodp.proc.322.202.2013.
Yamaguchi, A., et al. (2011), Progressive illitization in fault gouge caused by seismic slip propagation along a megasplay fault in the Nankai Trough, *Geology*, *39*, 995–998, doi:10.1130/G32038.1.